

Oriental Control of Electronic Coupling in Mixed-Valence, Binuclear Ruthenium(II)–Bis(2,2':6',2''-Terpyridine) Complexes

Andrew C. Benniston,¹ Anthony Harriman,^{*1} Peiyi Li,¹ Craig A. Sams,¹ and Michael D. Ward²

Molecular Photonics Laboratory, School of Natural Sciences, University of Newcastle, Newcastle upon Tyne, NE1 7RU, U.K., and Department of Chemistry, University of Sheffield, Sheffield, S3 7HF, U.K.

Received August 9, 2004; E-mail: anthony.harriman@ncl.ac.uk

The detailed analysis of intervalance charge-transfer (IVCT) absorption transitions has been instrumental in the development of electron-transfer theory.³ Using a simple but elegant theoretical model introduced by Hush,⁴ together with classical experimental studies provided by Creutz,⁵ Boxer,⁶ Launay,⁷ Hupp,⁸ and so forth,⁹ it has been possible to establish how the molecular architecture helps to control through-bond electronic coupling. Apart from solvent effects¹⁰ and the distance dependence,³ it has been shown that the electronic coupling matrix element (V_{DA}) between metal centers separated by a 4,4'-bipyridyl spacer decreases when methyl groups are substituted at the 2,2'-positions.¹¹ The magnitude of V_{DA} is restored if the spacer is forced to adopt a planar geometry.¹² These findings, taken together with recent quantum chemical calculations,¹³ indicate that V_{DA} for such systems depends critically on the torsion angle of the bipyridyl bridge. We now extend this work by reporting on the IVCT behavior of a set of binuclear ruthenium(II)–bis(2,2':6',2''-terpyridine) complexes where the geometry of the bridging biphenylene unit is constrained by a tethering strap of variable length (Figure 1).

The binuclear complexes, **C1**–**C4**, were prepared as the hexafluorophosphate salts and purified as described previously.¹⁴ Cyclic voltammetry studies carried out in acetonitrile containing 0.1 M tetra-*N*-butylammonium hexafluorophosphate as the background electrolyte showed that the two metal centers were oxidized with a half-wave potential ($E_{1/2}$) of +1.27 V versus Ag/AgCl. There was no obvious splitting of the oxidation peak and little, if any, variation in $E_{1/2}$ among the four compounds. These findings suggest that the metal centers are not in strong electronic communication. Relative to the mononuclear complex, the $E_{1/2}$ value for each of the binuclear complexes is raised by ~30 mV.¹⁵

Spectroelectrochemical studies made under controlled oxidation showed progressive absorption spectral changes across the UV, visible, and near-IR regions (Figure 2). In particular, stepwise oxidation results in the loss of the absorption associated with the intense ($\epsilon_{MLCT} \sim 30\,000\text{ M}^{-1}\text{ cm}^{-1}$) metal-to-ligand charge-transfer (MLCT) band found around 490 nm. Concomitant with this decreased absorptivity in the visible region is a steady increase in absorption around 800 nm. This latter absorption band, the precise location of which depends on the length of the tethering strap (see the Supporting Information), increases in intensity with increasing percent oxidation of the metal centers. The maximum intensity is reached when both metal centers are fully oxidized (i.e., 100%). As such, this new absorption band can be attributed to a ligand-to-metal charge-transfer (LMCT) transition.¹⁶ (The spectral properties assigned to the LMCT band are provided in the Supporting Information.) Typically, the band maximum is around 800 nm, and the molar absorption coefficient at the band maximum, ϵ_{LMCT} , is ~1500 $\text{M}^{-1}\text{ cm}^{-1}$ in acetonitrile at room temperature. Following the treatment of Crutchley et al.,¹⁶ we can best describe the LMCT

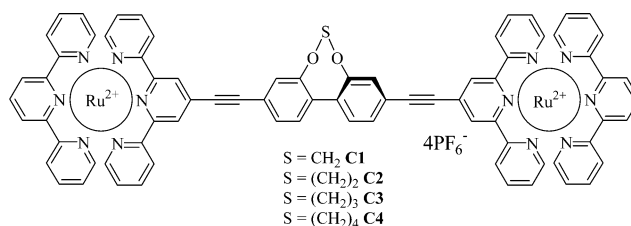


Figure 1. Structural representation of the binuclear ruthenium(II)–bis(2,2':6',2''-terpyridine) complexes, incorporating a dialkoxy-linked 4,4'-biphenylene unit.

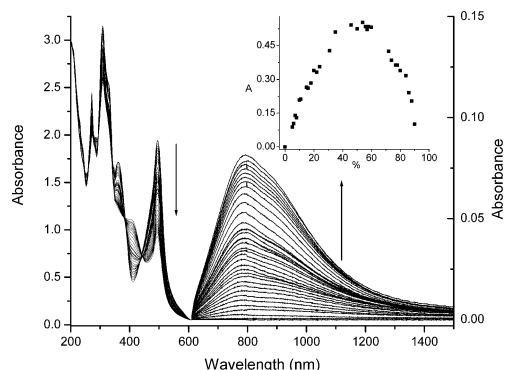


Figure 2. Absorbance changes in the UV–visible and near-IR regions following stepwise oxidation of **C1**. Inset shows relative absorbance of the IVCT band as a function of percent oxidation.

transition in terms of two overlapping Gaussian bands (see the Supporting Information).

Careful analysis of the LMCT region under conditions relating to partial oxidation of the metal centers reveals the presence of an additional absorption band lying at relatively low energy.¹⁶ For a given compound, the intensity of this latter band reaches a maximum at ~50% oxidation and decreases as the oxidation percent increases (see the Supporting Information). This finding strongly supports its assignment as the IVCT transition. The position of the band maximum (ν_{MAX}), the band half-width (fwhm), and the molar absorption coefficient at the band maximum (ϵ_{IVCT}) are sensitive to the length of the tethering strap (Table 1). As expected for an IVCT transition, the bands are weak, broad, and well-described in terms of a Gaussian profile.

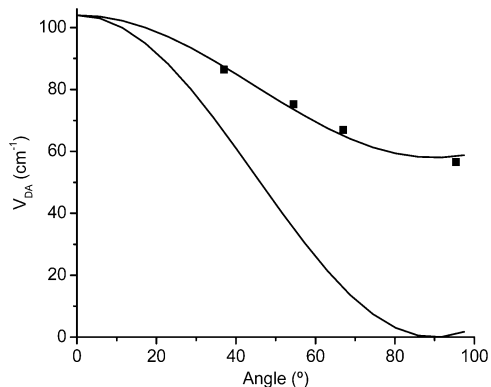
According to Hush,⁴ the IVCT spectra can be analyzed in terms of eq 1 in order to estimate V_{DA} for that compound.

$$V_{DA} = \frac{0.0205\nu_{MAX}}{R_{MM}} \sqrt{\frac{\epsilon_{MAX} fwhm}{\nu_{MAX}}} \quad (1)$$

Here, R_{MM} refers to the distance between the metal centers, as determined from molecular modeling. It is known that this distance

Table 1. Parameters Extracted from a Hush Analysis of the IVCT Transition Observed for the Various Strap Lengths

	ν_{MAX} (cm^{-1})	ϵ_{MAX} ($\text{M}^{-1}\text{cm}^{-1}$)	fwhm (cm^{-1})	$\times 10^3$ (f)	V_{DA} (cm^{-1})	angle (deg)	$1-\alpha^2$	ΔG_{R} (J mol^{-1})
C1	9775	305	3720	5.2	86	37	0.99992	9
C2	9925	185	4570	3.9	75	55	0.99994	7
C3	7570	270	3280	4.0	67	67	0.99992	7
C4	8180	220	2670	2.7	57	94	0.99995	3

**Figure 3.** Variation in the coupling element, V_{DA} , with torsion angle (■) for **C1–C4** and the best fit to eq 2. The other solid line is what is expected for the full angular dependence.

($R_{\text{MM}} = 25 \text{ \AA}$) is a crude approximation,⁶ but in the present case, it should remain constant throughout the series. The derived values for V_{DA} (Table 1) vary from ~ 85 to $\sim 55 \text{ cm}^{-1}$ as the tethering strap becomes longer.¹⁷ It should be stressed that, although the variation in V_{DA} is modest, the only difference among this series of compounds concerns the length of the dialkoxy strap. From the oscillator strengths (f) measured for these weakly coupled Class II systems,⁴ the extent of localization of the electron ($1-\alpha^2$) is essentially unity (Table 1).

The comproportionation constants ($K_{\text{C}} \sim 6$) calculated for varying degrees of oxidation are only slightly above those of the statistical limit¹¹ and show no obvious dependence on the length of the strap. Since the electrostatic contribution to K_{C} ($\Delta G_{\text{E}} = -265 \text{ J mol}^{-1}$) is expected to remain constant throughout the series, the observed invariance of K_{C} indicates that the mixed-valence species is not stabilized by way of extended electron delocalization (ΔG_{R}). In fact, the derived ΔG_{R} values show a progressive decrease as the strap length increases (Table 1), but the effect is almost insignificant.

A series of molecular dynamics simulations were carried out in an effort to establish likely conformations for the binuclear complexes (see the Supporting Information).¹⁸ It was found that the strap imposed a preferred angle for the lowest-energy conformation (Table 1), but that the structure was in dynamic fluctuation. There is a clear correlation between V_{DA} and the torsion angle, θ (Figure 3); in fact, V_{DA} favors a maximum at 0° and a minimum at 90° . This is expected on the basis of quantum chemical calculations,¹³ but the full impact of the angle dependence is not seen in our studies. Most likely, this is because internal fluctuations permit the biphenylene unit to sample a range of geometries, each with its own V_{DA} value.

The data can be fit to a generic expression for a damped 1D oscillation (Figure 3), for which there is a total V_{DA} of $\sim 105 \text{ cm}^{-1}$ for the planar geometry:

$$V_{\text{DA}} = V_0 + V_1 \cos^2 \Theta \quad (2)$$

The inherent coupling element $V_0 = 60 \text{ cm}^{-1}$ arises from the internal flexibility, while $V_1 = 45 \text{ cm}^{-1}$ represents the angle-dependent coupling element. A full molecular dynamics simulation in a solvent bath indicates that, for example, **C2** can access θ values ranging from 30 to 80° , and this accounts for the high V_0 value. A more-detailed description of the system, including additional compounds, will follow.

Acknowledgment. We thank the EPSRC (GR/23305) and the Universities of Newcastle and Sheffield for financial support.

Supporting Information Available: Figures showing the deconvolution of the near-IR spectral region of the LMCT and IVCT bands, LMCT spectra for the different compounds, the effect of oxidation percent on the absorbance of LMCT and IVCT bands, and an example of the variation in torsion angle, as obtained from the molecular dynamics simulations. This material is available free of charge via the Internet at <http://pubs.acs.org>.

References

- (1) University of Newcastle.
- (2) University of Sheffield.
- (3) Launay, J.-P. *Chem. Soc. Rev.* **2001**, *30*, 386.
- (4) (a) Hush, N. S. *Trans. Faraday. Soc.* **1961**, *57*, 557. (b) Hush, N. S. *Electrochim. Acta* **1968**, *13*, 1005.
- (5) (a) Creutz, C.; Taube, H. *J. Am. Chem. Soc.* **1969**, *91*, 3988. (b) Creutz, C.; Taube, H. *J. Am. Chem. Soc.* **1973**, *95*, 1086.
- (6) Bublitz, G. U.; Laidlaw, W. M.; Denning, R. G.; Boxer, S. G. *J. Am. Chem. Soc.* **1998**, *120*, 6068.
- (7) Patoux, C.; Launay, J.-P.; Beley, M.; Chodorowski-Kimmes, S.; Collin, J.-P.; Sauvage, J.-P. *J. Am. Chem. Soc.* **1998**, *120*, 3717.
- (8) Hupp, J. T. *J. Am. Chem. Soc.* **1990**, *112*, 1563.
- (9) (a) Hush, N. S. *Prog. Inorg. Chem.* **1967**, *8*, 391. (b) Creutz, C. *Prog. Inorg. Chem.* **1983**, *30*, 1.
- (10) (a) Brown, G. M.; Sutin, N. *J. Am. Chem. Soc.* **1979**, *101*, 883. (b) Cannon, R. D. *Chem. Phys. Lett.* **1977**, *49*, 299. (c) Creutz, C. *Inorg. Chem.* **1978**, *17*, 3723.
- (11) (a) Sutton, J. E.; Sutton, P. M.; Taube, H. *Inorg. Chem.* **1979**, *18*, 1017. (b) Sutton, J. E.; Taube, H. *Inorg. Chem.* **1981**, *20*, 3125.
- (12) Taube, H. *Ann. N.Y. Acad. Sci.* **1978**, *313*, 481.
- (13) Toutounji, M. M.; Ratner, M. A. *J. Phys. Chem. A* **2000**, *104*, 8566.
- (14) Benniston, A. C.; Harriman, A.; Li, P.; Sams, C. A. *Tetrahedron Lett.* **2003**, *44*, 4167.
- (15) Benniston, A. C.; Chapman, G. M.; Harriman, A.; Mehrabi, M.; Sams, C. A. *Inorg. Chem.* **2004**, *43*, 4227.
- (16) (a) Naklicki, M. L.; Crutchley, R. J. *J. Am. Chem. Soc.* **1994**, *116*, 6045. (b) Evans, C. E. B.; Yap, G. P. A.; Crutchley, R. J. *Inorg. Chem.* **1998**, *37*, 6161.
- (17) (a) Analysis by the Creutz–Newton–Sutin method, which does not depend on IVCT spectral properties, gave similar V_{DA} values: (b) Creutz, C.; Newton, M. D.; Sutin, N. *J. Photochem. Photobiol., A* **1994**, *82*, 47.
- (18) Molecular dynamics and geometry optimizations were carried out using Insight II. Partial charges were assigned using the ESFF force field. Optimized geometries were obtained using the Newton method, and molecular dynamics simulations were run up to 200 ps with a step function of 1 fs. Calculations were made in a solvent box using periodic boundary conditions and included the counterions.

JA0451968